

Video-Based Pedestrian Attribute Recognition

Zhiyuan Chen, Annan Li, and Yunhong Wang

Abstract—In this paper, we first tackle the problem of pedestrian attribute recognition by video-based approach. The challenge mainly lies in spatial and temporal modeling and how to integrating them for effective and dynamic pedestrian representation. To solve this problem, a novel deep recurrent neural network with hybrid pooling strategy is proposed. Since publicly available dataset is rare, a new large-scale video dataset for pedestrian attribute recognition is annotated, on which the effectiveness of both video-based pedestrian attribute recognition and the proposed new network architecture is well demonstrated.

Index Terms—Video-based pedestrian attribute recognition, convolutional neural networks, long short-term memory.

1 INTRODUCTION

PEDESTRIAN attribute, such as gender, age and clothing characteristics, has drawn a great attention recently due to its wide range of applications in intelligent surveillance system. It can be used for retrieving pedestrian and assisting other computer vision tasks, such as human detection [1], person re-identification [2], [3], [4], [5], [6], [7] etc.

In the past years, a lot of effort has been made to pedestrian attribute recognition. Layne et al. [2], Deng et al. [8] and Li et al. [3] use support vector machines to recognize pedestrian attribute, while AdaBoost is utilized by Zhu et al. [9]. Recently, Convolutional Neural Networks (CNN) have been adopted. Sudowe et al. [10] propose a jointly-trained holistic CNN model, while Li et al. [11] investigate CNN for both individual and group attributes. Liu et al. [12] introduce attention model to CNN-based pedestrian attribute recognition. Wang et al. [13], use recurrent learning for modeling the attribute correlations. Zhao et al. [14] further improve such approach by analyzing intra-group and inter-group correlations. Since clothing attribute is highly relevant to spatial location, Li et al. [15] use pose estimation for assistance.

Although demonstrate good performance, the above-mentioned methods are all based on static image. They are trained and evaluated on datasets with only one image per instance [8], [16], [17], [18], [19]. However, in a real-world surveillance scenario, consecutive image sequence is available. As can be seen from Figure 1 (a), a single shot of pedestrian (dashed rectangle) is not necessarily the most representative one for a specific attribute. Besides that sequential data can also provide strong temporal cues (see Figure 1 (b)), which are overlook in existing image-based approaches. It is reasonable that pedestrian attribute recognition should be tackled by video-based approach.

In this paper, A novel deep learning approach for video-based pedestrian attribute recognition is proposed. To our knowledge, it is the first one tackling pedestrian attribute recognition by video. Lack of data is the possible reason why existing approaches are limited to static image. To address this problem, we annotate a large-scale dataset of pedestrian image sequences with rich attribute. Experimental results



Fig. 1. Comparison between image and video based pedestrian attribute recognition. (a) Backpack is invisible in the frontal view, but can be clearly observed in other image of a sequence. (b) For a woman in dark color, it is difficult to classify whether she is wearing a skirt or shorts using one single image of limited resolution. However, the difficulty can be mitigated with the swinging of skirt.

clearly demonstrate that the proposed approach is very effective. Detailed contributions of this paper include:

- A large-scale pedestrian video dataset with rich attribute annotation is presented.
- A convolutional and recurrent architecture of deep neural network is proposed for pedestrian attribute recognition.
- We propose a novel pooling strategy for spatial-temporal modeling of the pedestrian.
- Extensive experiments are conducted and the results clearly show the superiority of video-based pedestrian attribute recognition.

The rest of this paper is organized as follows. The next section describes the annotated dataset. Then, Section 3 introduces the proposed video-based pedestrian attribute recognition approach. Experimental results are shown in Section 4 and conclusion is drawn in Section 5.

2 DATASET

Existing datasets for pedestrian attribute recognition such as PETA [8], RAP [16] and Market-1501 [17], [20] are mainly image-based. Fortunately, with the progress in video-based person re-identification (ReID), large-scale dataset of pedestrian image sequence becomes available. The Motion Anal-

Z. Chen, A. Li and Y. Wang are with School of Computer Science and Engineering, Beihang University, Beijing, China. E-mail:{dechen, liannan, yhwang}@buaa.edu.cn

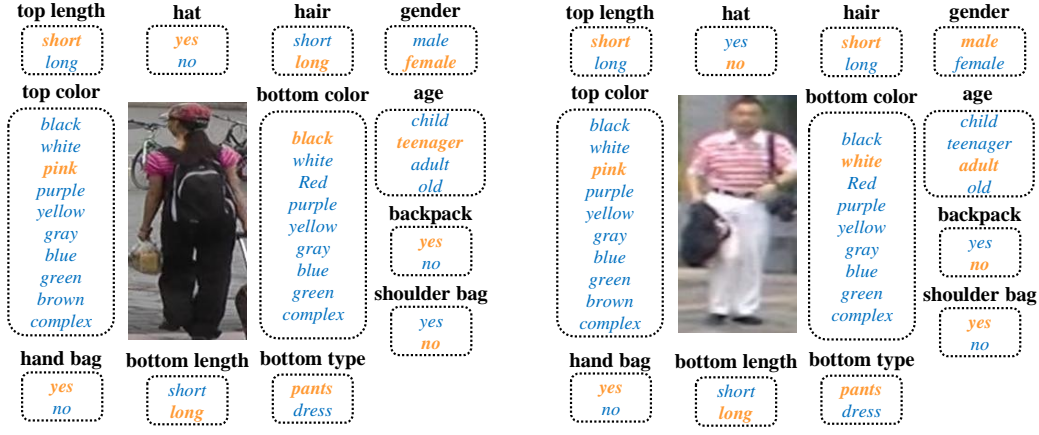


Fig. 2. Exemplar attribute annotation.

ysis and Re-identification Set (MARS) [21] is a newly released dataset, which consists of 20,478 tracklets from 1,261 different people captured by at least two cameras. MARS is an extension of Market-1501, they share the same identity. Although Lin et al. [20] provides identity-level attribute annotation for Market-1501, these annotations cannot be directly adopted to MARS for two reasons: Firstly, the correspondence between Market-1501 and MARS is not one-to-one, since there are more instances in MARS; Secondly, as can be seen from Figure 3, due to some temporal changes, even for the same people, some attribute appears while some attribute disappears. Therefore the identity-level annotation of Market-1501 is inaccurate for MARS.



Fig. 3. Examples of attribute change over time in MARS. A man puts on a backpack (left) and woman takes off her cardigan (right). Using the attributes annotated on a single frame for all the video instances of a pedestrian may incorporate errors.

To address the above-mentioned problem, we build a new dataset by re-annotating MARS using the attribute definition by Lin et al. [20]. As shown in Figure 2, there are 12 kinds of attributes are labeled for each tracklet in MARS dataset: gender (male, female), length of hair (long, short), length of tops/sleeve (long, short), length of bottoms (long, short), type of bottoms (pants, dress), wearing hat (yes, no), carrying shoulder bag (yes, no), carrying backpack (yes, no), carrying handbag (yes, no), nine bottom colors (black, white, red, purple, yellow, gray, blue, green, complex), ten top colors (black, white, pink, purple, yellow, gray, blue, green, brown, complex) and four kinds of ages (child, teenager, adult, old) which results in a total attribute number of 32. The attribute distributions are given in Figure 4. The dataset is published on <https://github.com/yuange250/MARS-Attribute>.

The proposed dataset provides not only a large-scale dataset for video-based pedestrian attribute recognition,

but also a benchmark for attribute-assisted person ReID. Because of the same identity and attribute definition, consistent comparison between image and video-based pedestrian attribute recognition can be achieved by directly comparing the performance on Market-1501 and this dataset (MARS).



Fig. 4. Statistics of annotated attributes.

3 APPROACH

In this section, we first describe the overall architecture of our spatial-temporal framework. Then we give a detailed introduction of the pooling strategy of the architecture.

3.1 Network Architecture

The overall architecture of our proposed model is illustrated in Figure 5. At the beginning of the network, we choose ResNet-50 [22] as the backbone model, and the outputs of the last flatten layer are used as the frame-level spatial features, then the network is separated into two channels:

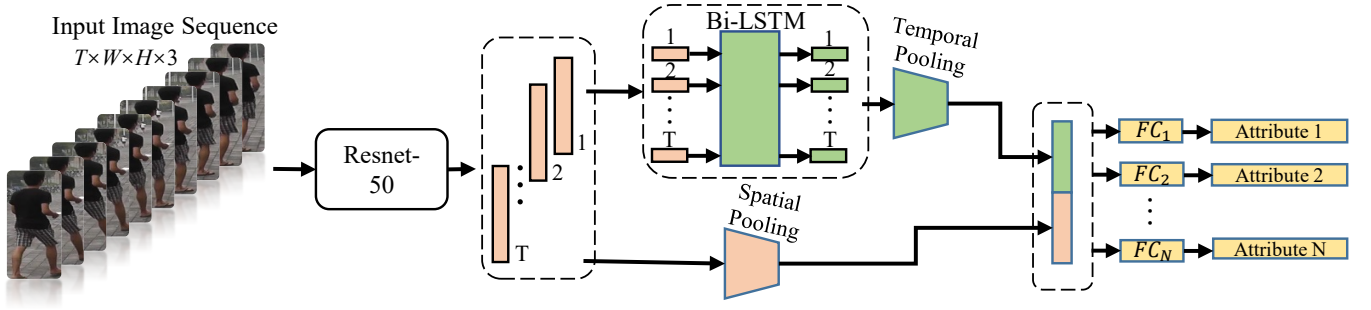


Fig. 5. Overall architecture of the proposed model. For each pedestrian image sequence, firstly the framework takes the image sequence as input and extract deep spatial features by using the Resnet-50 network, then the spatial features is processed by two saperated channels, one is the temporal channel highlighted in green color which extracts temporal features from the spatial feature sequence and intergrates the temporal features by temporal pooling, the other blow the temporal channel is the spatial pooling channel which intergrates the spatial features, nextly both the intergrated spatial feature and temporal feature will be concatenated into the final spatial-temporal feature, and at last the spatial-temporal feature will be utilized by N classifiers to predict N attributes.

i.e. the temporal modeling channel and the spatial pooling channel respectively. With the frame-level features, a bi-directional Recurrent Neural Networks (RNN) [23], [24] with Long Short-Term Memory (LSTM) [24], [25] is adopted in the temporal modeling channel. Conventional RNN tends to focus on the latter input, however the most representative frame for a specific attribute is not necessarily at the end of a sequence. Since the bi-directional structure of RNN can output relative balanced LSTMs over time, it is adopted as the temporal feature extractor. After the bi-directional LSTM (Bi-LSTM) modeling the feature is further compressed by a temporal pooling layer. The spatial channel is simply a pooling layer, whose results are concatenated with temporal features for consequent attribute classification.

Let $I = \{I_1, I_2, \dots, I_n\}$ be the input image sequence or a tracklet, where n , w and h are the frame number, image width and height respectively, and we choose $w, h = 256$ in practice. Using the spatial feature extractor Resnet-50, each frame is represented by a 8,192 dimensional vector. Consequently, the $n \times w \times h \times 3$ input tensor is converted into a two dimensional matrix $S = \{S_1, S_2, \dots, S_n\}$, $S \in \mathbb{R}^{n \times 8192}$.

Then the spatial feature vector is processed by the two channels respectively. The temporal channel first generates LSTMs $T = \{lstm(S_1), lstm(S_2), \dots, lstm(S_n)\}$ for every input frame. Then LSTM feature $T \in \mathbb{R}^{n \times 8192}$ is converged into a vector $T^{pool} \in \mathbb{R}^{1 \times 8192}$ by a temporal pooling layer. Meanwhile, the input feature S is pooled into a vector $S^{pool} \in \mathbb{R}^{1 \times 8192}$ in the spatial channel. The details of pooling strategy will be discussed in Section 3.2. At last, the temporal feature vector T^{pool} and spatial feature vector S^{pool} are concatenated and fed into fully connected layers to achieve the attribute classification results.

We evaluate the influence of both spatial and temporal streams in term of attributes recognition accuracy in Section 4, and the results shows that combining both spatial and temporal features is the best choice for video-based pedestrian attributes recognition.

3.2 Two-Stream Pooling Strategy

Although ResNet-50 is able to capture effective spatial information from each single frame, and the following bi-

directional LSTM can further extract useful temporal features. However, we find that sole temporal modeling is insufficient for a reliable attribute classifier, since LSTM tends to focus on the inter-frame changes. In other words, discriminative spatial information might be overlook by LSTM. As can be seen from Figure 1 and Figure 2, visual appearance in some key frame is sufficient for determining the existence of an attribute. The intra-frame spatial feature and the inter-frame temporal feature are complementary for recognizing the pedestrian attribute. Therefore, it is better to integrate them together.

Inspired by the pooling strategy in [26], we investigate both max-pooling and mean-pooling for aggregating the feature vectors into a more reliable one. Applied them to spatial feature S and temporal feature T respectively, four different combinations can be derived. The experimental comparisons will be presented in Section 4.2.

4 EXPERIMENTS

In this section, firstly we give a brief description about the train/test partition of the annotated MARS dataset as well as some training settings in the experiments. Then we evaluate the effect of four different pooling strategies and the best pooling strategy is proposed according to the experiment result. Lastly ablation experiment shows the different influence of the spatial channel and the temporal channel in the proposed method, which also prove the effectiveness of the spatial-temporal feature aggregation.

4.1 Settings

We follow the origin train/test partition rule of MARS [21]. The training set consists of 8,298 tracklets from 625 people, while the rest 8,062 tracklets corresponding to 626 pedestrians make up the test set. There is no shared identity in the two sets.

The training progress include two stages. Firstly the backbone network resnet-50 is fine-tuned in an image-based way on the annotated MARS dataset. Then the two-channel spatial-temporal modeling network (right part in Figure 5) is trained using the feature given by the backbone network. Mean Squared Error (MSE) is chosen as the loss function

TABLE 1
Comparisons of recognition accuracy on MARS datasets.

Pooling Method		top color	bottom color	age	top length	bottom length	shoulder bag	back pack	hat	hand bag	hair	gender	bottom type	Mean
Spatial	Temporal													
mean	mean	0.7193	0.7105	0.8355	0.9422	0.9366	0.8092	0.8933	0.9819	0.8668	0.8877	0.9166	0.9390	0.8701
mean	max	0.7184	0.7114	0.8356	0.9441	0.9377	0.8100	0.8944	0.9819	0.8674	0.8884	0.9189	0.9391	0.8706
max	mean	0.7026	0.7009	0.8296	0.9083	0.9262	0.7518	0.8075	0.9452	0.6455	0.8597	0.8937	0.8869	0.8215
max	max	0.7040	0.7000	0.8290	0.9064	0.9235	0.7516	0.8143	0.9453	0.6500	0.8559	0.8894	0.8856	0.8212
spatial only		0.6857	0.6894	0.8342	0.9451	0.9366	0.8097	0.8940	0.9810	0.8663	0.8879	0.9176	0.9377	0.8654
temporal only		0.6694	0.6596	0.8371	0.9418	0.9328	0.7976	0.8900	0.9784	0.8614	0.8820	0.8923	0.9354	0.8565
APR [20]		0.7340	0.6991	0.8708	0.9366	0.9332	0.7507	0.8279	0.9713	0.8298	0.8365	0.8645	0.9146	0.8533

and Stochastic Gradient Descent (SGD) with a learning rate 0.002 is selected as the optimizer in both stages.

4.2 Pooling Strategy

As mentioned in Section 3.2, both max-pooling and mean-pooling are investigated, which results in four combinations. The experimental comparisons are shown in Table 1. As can be seen, spatial mean-pooling considerably outperforms max-pooling. As to the temporal pooling, when spatial mean-pooling is combined, maximum operation achieve consistent better results on all attributes except for *top color*. Considering that max-pooling tends to focus on the salient features and mean-pooling compress the information in a relatively mild way, the results imply that evenly preserving spatial details and abstract salient temporal feature helps improving the performance.

The phenomenon is consistent with the observations shown in Figure 1. The key frames clearly showing the appearance of backpack and skirt flare are the most representative ones. Picking them out is relevant to the maximum pooling operation. It also shows that sole temporal feature is insufficient, highlighting the representativeness of key frames needs necessary spatial cues. The pedestrian attributes annotated in our dataset can be relevant to any part of the body (see Figure 2). In other words, a region important to some attributes is not necessarily the same important to others. It is reasonable that emphasizing some specific spatial region might lead to detail loss. That is the possible explanation why max-pooling is not as good as mean-pooling for spatial feature.

4.3 Comparison with Image-Based Approaches

The key contribution of this work is the introduction of video-based approach to pedestrian attribute recognition. To demonstrate its superiority, two series of experiments are conducted. The spatial channel in our framework actually can be viewed as an image-based attribute recognition approach, which is applied to a set-to-set scenario and uses the average one to represent the whole set. Therefore, the first series of comparison is achieved by comparing the performance of single spatial channel and that of the combined one. Since the combination of spatial mean-pooling and temporal max-pooling achieves the best results, it is adopted in this experiment.

The results of single channels are shown in the middle block of Table 1. For single channels, although not as good as spatial modeling, temporal modeling can achieve similar performance. It shows that the proposed Bi-LSTM

is quite effective. The combined spatial-temporal modeling outperforms the spatial channel on all attribute except for the *top length*. It demonstrates both the effectiveness of the proposed two-stream architecture and the superiority of video-based approach in recognizing pedestrian attribute.

Because the people in Market-1501 [17] and MARS [21] are the same and we followed the attribute definition of Market-1501 [20] in annotating MARS, comparison between image and video-based approach can be achieved by directly comparing the results reported on Market-1501 and MARS. It should be pointed out that the train/test set partitions of Market-1501 and MARS are different. Since multiple images of an instance are available, MARS can provide more information than Market-1501. However, the image sequence of MARS are obtained by automatic tracking and clustering. Therefore, noisy and low-quality samples are inevitably included in MARS. Although, Market-1501 only has one image per instance, this image is manually selected. In other words, the average quality and representativeness of Market-1501 is far better than MARS.

The Attribute-Person Recognition (APR) Network by Lin et al. [20] is the state-of-the-art on Market-1501. Its results are shown in the bottom row of Table 1. As can be seen, except for *top color* and *age*, our method outperforms APR in all the rest attribute. The overall accuracy is 0.8706 vs 0.8533, which clearly proves the advantage of our method. As above-mentioned, video brings not only adequate information but also the noises and variations. Because of the illumination change, for a video clip or image sequence in MARS, many frames are very dark, which results in low contrast of color. Therefore, it is not surprising that single image based method can get a better results in color-relevant recognition. As to age, pose variations is the possible explanation. With limited resolution, age difference is possibly relevant to the holistic clothing and hair style. The overall appearance of a people is easily affected by pose.

5 CONCLUSION

In this paper, we first study pedestrian attribute recognition with video-based approach. A new large-scale dataset for video-based pedestrian attribute recognition is presented. We also proposed a novel spatial-temporal modeling network architecture with hybrid pooling strategy. Experiments show that video-based approach is better than image-based method in recognizing pedestrian attribute and the proposed architecture is very effective.

ACKNOWLEDGMENT

This work was supported by The National Key Research and Development Plan of China (Grant No.2016YFB1001002).

REFERENCES

- [1] Y. Tian, P. Luo, X. Wang, and X. Tang, "Pedestrian Detection aided by Deep Learning Semantic Tasks," in *IEEE Conference on Computer Vision and Pattern Recognition*, 2015, pp. 5079–5087.
- [2] R. Layne, T. M. Hospedales, and S. Gong, "Person Re-identification by Attributes," in *British Machine Vision Conference*, 2012.
- [3] A. Li, L. Liu, K. Wang, S. Liu, and S. Yan, "Clothing Attributes Assisted Person Re-identification," *IEEE Transactions on Circuits and Systems for Video Technology*, vol. 25, no. 5, pp. 869–878, 2015.
- [4] J. Zhu, S. Liao, D. Yi, Z. Lei, and S. Z. Li, "Multi-label CNN Based Pedestrian Attribute Learning for Soft Biometrics," in *International Conference on Biometrics*. IEEE, 2015, pp. 535–540.
- [5] T. Matsukawa and E. Suzuki, "Person Re-Identification Using CNN Features Learned from Combination of Attributes," in *International Conference on Pattern Recognition*, 2016, pp. 2428–2433.
- [6] C. Su, F. Yang, S. Zhang, Q. Tian, L. S. Davis, and W. Gao, "Multi-Task Learning with Low Rank Attribute Embedding for Multi-Camera Person Re-Identification," *IEEE transactions on pattern analysis and machine intelligence*, vol. 40, no. 5, pp. 1167–1181, 2018.
- [7] J. Wang, X. Zhu, S. Gong, and W. Li, "Transferable Joint Attribute-Identity Deep Learning for Unsupervised Person Re-Identification," in *IEEE Conference on Computer Vision and Pattern Recognition*, 2018, pp. 2275–2284.
- [8] Y. Deng, P. Luo, C. C. Loy, and X. Tang, "Pedestrian Attribute Recognition At Far Distance," in *ACM International Conference on Multimedia*, 2014, pp. 789–792.
- [9] J. Zhu, S. Liao, Z. Lei, D. Yi, and S. Z. Li, "Pedestrian Attribute Classification in Surveillance: Database and Evaluation," in *IEEE International Conference on Computer Vision Workshops*, 2013, pp. 331–338.
- [10] P. Sudowe, H. Spitzer, and B. Leibe, "Person Attribute Recognition with a Jointly-Trained Holistic CNN Model," in *IEEE International Conference on Computer Vision Workshops*, 2015, pp. 329–337.
- [11] D. Li, X. Chen, and K. Huang, "Multi-attribute Learning for Pedestrian Attribute Recognition in Surveillance Scenarios," in *Asian Conference on Pattern Recognition*, 2015, pp. 111–115.
- [12] X. Liu, H. Zhao, M. Tian, L. Sheng, J. Shao, S. Yi, J. Yan, and X. Wang, "HydraPlus-Net: Attentive Deep Features for Pedestrian Analysis," in *IEEE International Conference on Computer Vision*, 2017, pp. 350–359.
- [13] J. Wang, X. Zhu, S. Gong, and W. Li, "Attribute Recognition by Joint Recurrent Learning of Context and Correlation," in *IEEE International Conference on Computer Vision*, 2017, pp. 531–540.
- [14] X. Zhao, L. Sang, G. Ding, Y. Guo, and X. Jin, "Grouping Attribute Recognition for Pedestrian with Joint Recurrent Learning," in *International Joint Conference on Artificial Intelligence*, 2018, pp. 3177–3183.
- [15] D. Li, X. Chen, Z. Zhang, and K. Huang, "Pose Guided Deep Model for Pedestrian Attribute Recognition in Surveillance Scenarios," in *IEEE International Conference on Multimedia and Expo*, 2018, pp. 1–6.
- [16] D. Li, Z. Zhang, X. Chen, H. Ling, and K. Huang, "A Richly Annotated Dataset for Pedestrian Attribute Recognition," *arXiv preprint arXiv:1603.07054*, 2016.
- [17] L. Zheng, L. Shen, L. Tian, S. Wang, J. Wang, and Q. Tian, "Scalable Person Re-identification: A Benchmark," in *IEEE International Conference on Computer Vision*, 2015.
- [18] H. U. Cheng, L. Chen, X. Zhang, and S. Y. Sun, "Pedestrian attribute recognition based on convolutional neural network in surveillance scenarios," *Modern Computer*, 2018.
- [19] M. S. Sarfraz, A. Schumann, Y. Wang, and R. Stiefelhagen, "Deep view-sensitive pedestrian attribute inference in an end-to-end model," 2017.
- [20] Y. Lin, L. Zheng, Z. Zheng, Y. Wu, and Y. Yang, "Improving person re-identification by attribute and identity learning," *arXiv preprint arXiv:1703.07220*, 2017.
- [21] L. Zheng, Z. Bie, Y. Sun, J. Wang, C. Su, S. Wang, and Q. Tian, "MARS: A Video Benchmark for Large-Scale Person Re-identification," in *European Conference on Computer Vision*, 2016.
- [22] K. He, X. Zhang, S. Ren, and J. Sun, "Deep Residual Learning for Image Recognition," in *IEEE Conference on Computer Vision and Pattern Recognition*, 2016, pp. 770–778.
- [23] M. Schuster and K. K. Paliwal, "Bidirectional Recurrent Neural Networks," *IEEE Transactions on Signal Processing*, vol. 45, no. 11, pp. 2673–2681, 1997.
- [24] A. Paszke, S. Gross, S. Chintala, G. Chanan, E. Yang, Z. DeVito, Z. Lin, A. Desmaison, L. Antiga, and A. Lerer, "Automatic Differentiation in PyTorch," in *Neural Information Processing Systems Workshop*, 2017.
- [25] S. Hochreiter and J. Schmidhuber, "Long Short-Term Memory," *Neural Computation*, vol. 9, no. 8, pp. 1735–1780, 1997.
- [26] N. McLaughlin, J. M. D. Rincon, and P. Miller, "Recurrent Convolutional Network for Video-Based Person Re-identification," in *IEEE Conference on Computer Vision and Pattern Recognition*, 2016, pp. 1325–1334.